NOTICE

CERTAIN DATA CONTAINED IN THIS DOCUMENT MAY BE DIFFICULT TO READ IN MICROFICHE PRODUCTS.

Conf-9110311--1

PNL-SA--19782

DE92 004515

CRACK-TIP CHEMISTRY MODELING OF STAGE I STRESS CORROSION CRACKING

R. H. Jones
E. P. Simonen

October 1991

Presented at the
Parkins Symposium on Fundamentals
of Stress Corrosion
October 20-24, 1991
Cincinnati, Ohio

Work supported by
the U.S. Department of Energy
under Contract DE-AC06-76RLO 1830

Pacific Northwest Laboratory
Richland, Washington 99352

DISCLAIMER

PNL-SA-8757

CRACK TIP CHEMISTRY MODELING OF STAGE I STRESS CORROSION CRACKING

R. H. Jones and E. P. Simonen
Pacific Northwest Laboratory
Richland, Washington 99352[a]

Abstract

Stage I stress corrosion cracking usually exhibits a very strong K dependence with Paris law exponents of up to 30. Model calculations indicate that the crack velocity in this regime is controlled by transport through a salt film and that the K dependence results from crack opening controlled salt film dissolution. An ionic transport model that accounts for both electromigration through the resistive salt film and Fickian diffusion through the aqueous solution was used for these predictions. Predicted crack growth rates are in excellent agreement with measured values for Ni with P segregated to the grain boundaries and tested in 1N H_2SO_4 at +900 mV. This salt film dissolution may be applicable to stage I cracking of other materials.

[a] Work supported by the U.S. Department of Energy under contract DOE-AC06-76RLO 1830

Introduction

The crack velocity-stress intensity relationship induced by stress corrosion cracking (SCC) in a wide variety of materials exhibits a threshold, and stage I and stage II regimes. The threshold, referred to as K_{ISCC}, is the stress intensity at which measurable crack extension occurs. Stage I is the regime in which the crack velocity exhibits a very strong dependence on stress intensity and stage II is the regime in which the crack velocity exhibits a very weak and sometimes neglible dependence on stress intensity.

The stage I regime plays a critical role in SCC, and yet most of the theoretical and experimental effort has been focused on K_{ISCC} and stage II. The slope of the stage I regime is important for determining design stresses to avoid SCC and for life prediction of a material should SCC be unavoidable. For components that must perform for extended periods, the stage I slope is a critical parameter because it defines the "long-term" K_{ISCC}. A laboratory defined K_{ISCC}, determined in hours, will approach the "long-term" K_{ISCC} with increasing stage I slope. The slope of the stage I regime is also a factor in life prediction because the crack velocity can increase by several orders of magnitude in this regime. The total impact on component life will be a function of incubation time, crack initiation time, transition from short crack to long crack electrochemistry and mechanics, and then crack growth as defined by conventional long crack K_{ISCC}, stage I and stage II.

Stage I behavior of materials has received very little experimental or theoretical emphasis. Stage I behavior is difficult to measure experimentally because of the strong stress intensity dependence where the velocity may increase by an order of magnitude with only a 1-2 MPa/m increase in the stress intensity, thus making stage I a very transient phenomenon. Also, because of the rapid increase in crack velocity, the velocity is determined from very small crack extensions. This results in greater scatter in the data because velocities are based on a relatively small sampling of the material and are not an average over a range of microchemical and microstructural variations. Theoretical emphasis has been placed in the electrochemical, mechanical, and microstructural/microchemical aspects of K_{ISCC} and stage II cracking. Most theoretical studies have not considered the stress or stress intensity aspects of SCC but have emphasized the physical processes involved. It is quite conceivable that these processes are involved to different degrees in K_{ISCC}, stage I and stage II cracking, but quantitative descriptions of the crack velocity-stress intensity relationships in stage I are absent from the literature.

Because of the distinctiveness and significance of this regime, an analytical description of stage I is of considerable value. This description will also enhance our understanding of K_{ISCC} and stage II SCC regimes. The purpose of this paper is to report on a modeling effort to describe the stage I behavior of Ni tested in 1N H_2SO_4 based on modifications to a crack tip chemistry model developed by Danielson, Oster, and Jones (1).

Background

Experimental crack velocity-stress intensity data for SCC is presented in one of the two following formulas:

$$da/dt = AK^m \quad (1)$$

or
$$\log da/dt = \log D + BK \quad (2)$$

Stage I would exhibit a linear da/dt versus K relationship with a log-log plot or semi-log plot if either equation 1 or 2 applies, respectively. However, in many cases the data is not sufficiently well described and the range of K is small so the data can be described by either relationship. An example is shown in Figure 1 where the stage I crack growth rate behavior of Fe tested in Na_2SO_4 at +1.25 V (SCE) is shown to fit both relationships. From this data one relationship is not clearly preferred over the other. Therefore, in considering an analytical description for stage I stress intensity dependence, both equations 1 and 2 must be considered until better data is available.

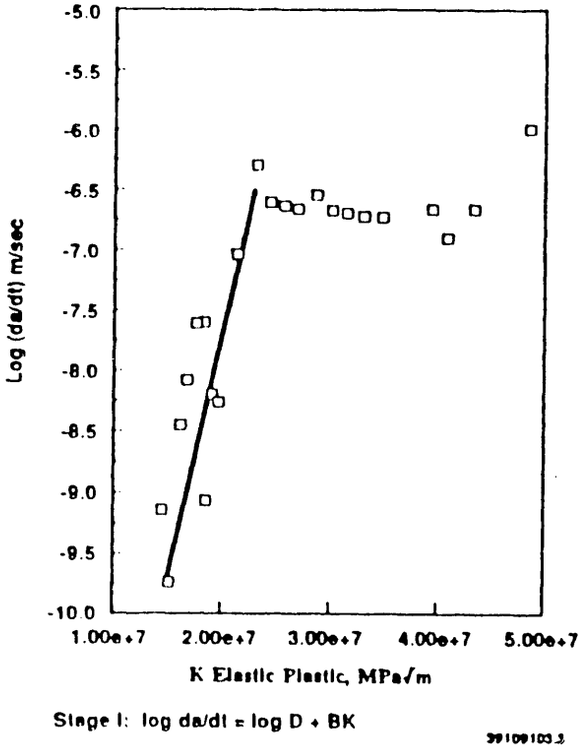

Figure 1. Stress Corrosion Crack Velocity versus Stress Intensity of Fe tested in 1M Na_2SO_4 at 1.25 V (SCE) a) log velocity versus K, and b) log velocity versus log k.

Examples of m and B values, equations 1 and 2, describing the slope of the stage I regime are given in Table 1 (2-12). In general, high values of m correspond to high values of B but the correspondence is imperfect probably because the data is imperfect. The m values for Type 304 SS range from 7 to 24; for Ni it is 11; for an aluminum alloy it is 19; and for iron tested in $Ca(NO_3)_2$ it was 4, while for Fe tested in Na_2SO_4 it ranged from 11 to 30. Sample geometry, compliance, loading method (increasing, constant or decreasing load), and sensitivity of crack measuring equipment are all factors that affect the accuracy of the data presented in Table 1. In spite of uncertainties in this data, there is an apparent trend in the Type 304 SS data where m is less than 10 for tests in pure water, 8-14 in Na_2SO_4, 11-17 in $Na_2S_2O_3$ and 24 for 22% NaCl. This trend suggests an increasing value of m with increasing effectiveness and concentration of critical species.

There has not been a model specifically developed for stage I behavior which includes the stress intensity as a variable, though there are a number of stress corrosion cracking models that do have stress intensity as a variable. These relationships are summarized in Table 2.

Andresen (13) has recently expanded on Ford's (14) stress corrosion crack growth rate-strain rate model and expressed the crack growth rate by Eq. 2-1, Table 2, where A and n come from Eq. 3 below:

$$da/dt = A \dot{e}_{ct}^{n} \qquad (3)$$

and $\dot{e}_{ct}$ is the crack tip strain rate and n is the exponent. A value of n equal to 0.76 was given by Andresen (13) while Ford (14) has assumed n to be 0.5. The crack growth rate is proportional to K to the 1.9 to 3.4 power based on n of 0.5 to 0.76.

These values of m are substantially less than those observed experimentally, as shown in Table 1, and are more consistent with the stress intensity dependence observed in the stage II regime. However, the rate-controlling step in the stage II regime is thought to be either ion transport in the crack electrolyte or the environment-crack tip reaction rate and not the passive film rupture rate as assumed by the Ford/Andresen analysis.

Table 1. Summary of Experimental Stage I Crack Growth Parameters m and B.

Material	Test Condition	m	B	Reference
304SS	Sensitized 97°C, 1.5 ppm 0_2	7	0.14	3
304SS	Sensitized 99°C, 22% NaCl	24	1.2	4
304SS	25°C, $6x10^{-4}$m $Na_2S_2O_3$	11	0.26	5
304SS	Sensitized 90°C, 15ppm $Na_2S_2O_3$	17	0.25	10
304SS	Sensitized, 250°C 10^{-2}m, Na_2SO_4	8	0.18	6
304SS	Sensitized, 289°C 10^{-3}m, Na_2SO_4	14	0.8	3
Ni + P	25°C, 1N Na_2SO_4 900 mV (SCE)	10	0.33	2
7079-1651 Al	25°C, Saturated NaCl	19	1.3	7
Fe	60°C, 55% $Ca(NO_3)_2$ + 750 mV (SCE)	4	0.11	11
Fe and Fe + P	25°C, 1M Na_2SO_4 +750-1250 mV (SCE)	11-30	0.34-1.0	12
Mild Steel	92°C, 33% NaOH E_{corr}	7	0.16	8
Brass	23°C, Ammoniacal Copper Sulfate (pH=7)	1.8	0.098	9

Table II. Summary of Predicted Stage I Crack Growth Parameter m

Material	Crack Growth Model	Eq. No.	m	Reference
304SS	$da/dt = [1.5\times10^{-8} K^{2.8}(A)^{1/n}]^{2n/2-n}$	2-1	1.9-3.4	13
Steel	$da/dt = e_c k\beta/sf(K) \ln(1-G)$	2-2	25	15
304SS	$da/dt = k' K^{p/\eta}$	2-3	p/η	16
304SS	$da/dt = \frac{MI_0}{2\rho_m Z F A_{crack}}$	2-4	dependent on K	17
Brass	$da/dt = A \exp\{[Q + f(K)]/RT\}$	2-5		9
Glasses	$da/dt = (da/dt)_0 a (H_2O) \exp\{(E^* + bK_I)/RT\}$	2-6		18

Newman (15) presented a film rupture stress corrosion model for steel in sodium hydroxide, Eq. 2-2, Table 2, in which he assumed that crack extension was limited to the thickness of the corrosion product film, l_c, which fractured in a time period, t_c, determined by the stress intensity and hence the crack tip strain rate. The crack velocity was expressed very similarly to the equation given by Vermilyea: (16)

$$da/dt = l_c/t_c. \tag{4}$$

The parameters l_c and t_c are interdependent with l_c depending on the strain rate and hence t_c. The expression for l_c was given as

$$l_c = e_c k/sf(k) \tag{5}$$

where e_c is the film rupture strain, k is a stress relaxation constant, s is a constant that relates the strain rate to the stress, and f(K) is a function of stress intensity. The expression for the critical strain, e_c, was given as

$$e_c = s\, f(K)\, v\,[1 - \exp(-\beta t_c)]/K\beta \tag{6}$$

where v is the initial corrosion rate, and β is the passivation rate constant. Solving Eq. 6 for t_c and substituting Eq. 6 and 7 into Eq. 5 gives the following relationship for the crack velocity:

$$da/dt = -e_c k \beta / s f(K) \ln(1-G) \tag{7}$$

where G is equal to $e_c k \beta / s f(K) v$. Eq. 7 is valid for the following values: $0 < G < 1$. Newman solved this relationship numerically and obtained curves for the crack velocity versus K for f(K) proportional to K and K^2. The two functions for K result in similar-shaped curves with K^2 dependence giving a slightly higher threshold value; however, the predicted slope, m, of the stage I regime was 25 for both cases. Newman concluded that the stress corrosion model was consistent with experimental data, but no comparison was made between calculated and experimental crack velocity-stress intensity relationships. The predicted slope of the stage I regime is within the range observed for Fe and mild steel but is near the upper end of the range of 4-30.

Vermilyea (16) considered the effect of the stress intensity and the solution chemistry by proposing that the relationship between crack velocity and stress intensity has the following form:

$$da/dt = k' C K^p \quad (8)$$

where k' is a constant and C is the concentration of some species in the crack tip solution. Then, assuming that the difference between the crack tip and mouth concentration is a function of crack velocity, he obtained the following relationship for crack velocity:

$$da/dt = k'' K^{p/\eta} \quad (9)$$

where η is a small constant in the crack tip concentration/crack velocity relationship and which Vermilyea considers to have a value of about 0.1. He suggested that small changes in η and hence in the crack tip chemistry could have large effects on the stress-intensity dependence of the crack velocity, which could explain the values of m ($m = p/\eta$) given in Table 1 for Type 304 SS. A systematic study of crack tip chemistry effects on the parameter m has not been carried out, but the data in Table 1 suggest that for sensitized Type 304SS m is less than 10 for high temperature water, 8-14 for Na_2SO_4, 11-17 for $Na_2S_2O_3$, and 24 for 22% NaCl. Increasing values of m suggest decreasing values of η in Vermilyea's model; behavior results from increasing concentrations of a critical species at the crack tip for a given crack velocity. Further work under more controlled conditions is needed to determine whether Vermilyea's theory is valid.

A recently published crack tip chemistry based model by Macdonald and Urquidi Macdonald (17) for IGSCC of Type 304 SS suggests that the stress intensity dependence results from a combination of the passive film rupture rate and crack opening. In essence, this model relates the crack tip potential to the stress intensity through the balance of the positive current produced by the crack with the reduction of oxygen at the external crack surfaces. The functional form of this equation is given by Eq. 2-4 in Table 2, where

$$I_c = f\{\exp[\ln(K^2)]\} \quad (10)$$

and M is the composition-weighted atomic weight, F is Faradays constant, ρ_m is the density of the metal, z is the composition weighted oxidation state and A_{crack} is the area of the crack at the crack mouth. A plot of equation 2-4 is given in Figure 2 where the results fit a form of $\log da/dt = A + BK^2$ with a threshold less than 1 $MPa\sqrt{m}$. Equation 2-4 predicts a rapidly increasing velocity with K at low stress intensities with a lesser increase in velocity at higher stress intensities. This model also predicts a K_{Iscc} of 0 $MPa\sqrt{m}$. Experimental values for K_{Iscc} for Type 304 SS are approximately 20-30 $MPa\sqrt{m}$ so this model clearly misrepresents the process controlling K_{Iscc}. Equation 2-4 suggests a continuous transition from stage I to stage II with an m value ranging from large to small depending on the value of K. Experimental da/dt versus K curves for Type 304 SS do resemble the calculated curve shown in Figure 2 (5,10) with exception to K_{Iscc}; however, a model that does not correctly describe K_{Iscc} is probably not a physically complete description of stage I. The approach used by Macdonald and Urquidi-Macdonald may be correct but it does not appear to account for the Stage I behavior.

Lee and Tromans(9) found that the crack velocity-stress intensity relationship for a cold-worked brass tested in an ammoniacal copper sulfate

solution could be described by a chemical rate equation, Eq. 2-5, which is of the form given by Eq. 2, where Q was 48.9 kJ/mole at K = 0 and f(K) was

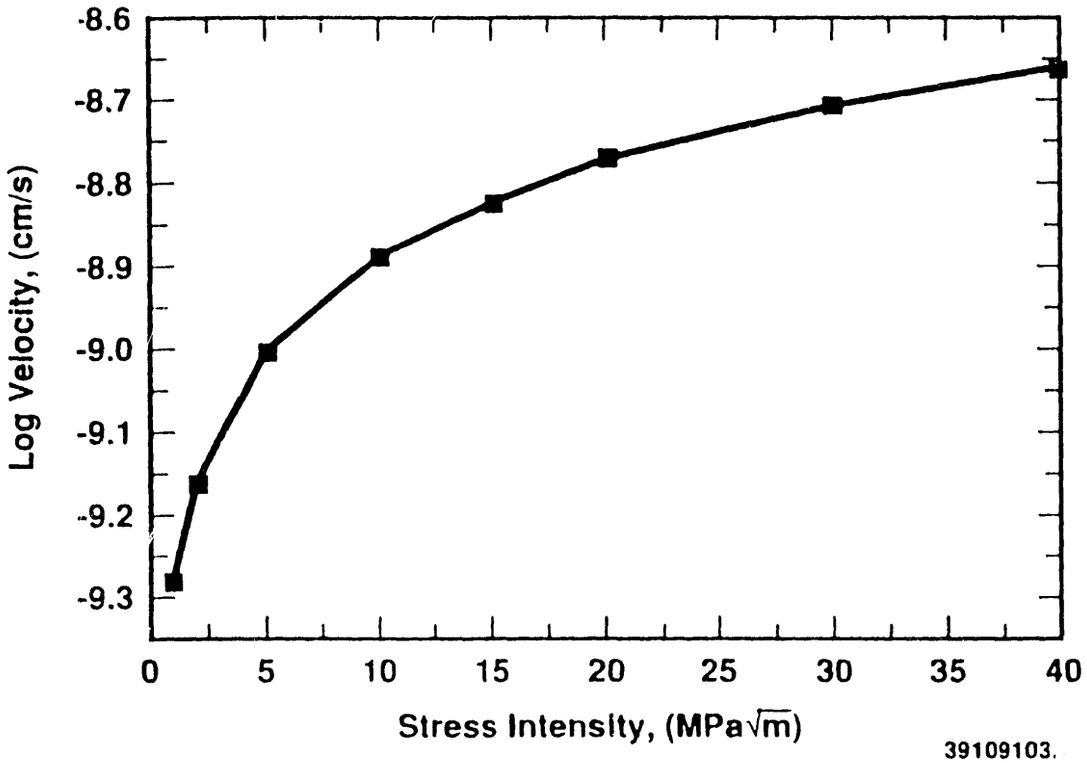

Figure 2. Effect of stress intensity (K_I) on crack velocity (17) [O_2] = 0.02 ppm, l = 1 cm, [NaCl] = 10^{-1} mol/cm^3, T = 573.15K. Other parameters are as listed in Ref. 17.

linear with K. The experimental data for crack velocity-stress intensity gives a value of m of 1.8, which is the smallest value given in Table 1.

A chemical rate equation has also been used by Freiman (18) to describe the SCC behavior of glasses, Eq. 2-6. Stress corrosion cracking of glasses results from the reaction of the environment with the highly strained bonds of the solid at the crack tip. This reaction is comparable to hydrogen or liquid metal embrittlement in metals since a corrosion product is not a necessary step in the process. The stress dependence results from the applied stress intensity and is expressed in Eq. 2-6 as being a linear function of K in the exponential term. This K dependence is similar to one used by Lee and Fromans (9).

Salt Film Dissolution Model

Danielson et al.(1) have noted that for low stress intensities, and hence low crack opening angles, high ion concentrations result from crack wall corrosion and from restricted transport of ions to the crack mouth. Salt formation is predicted if the ion concentration produced by anodic dissolution exceeds the solubility limit. Critical crack opening angles associated with the stage I-II transitions, which correspond to the formation of resistive salts at a crack tip, can be calculated. The salt resistance results in a potential (IR) drop, low crack tip corrosion rates, and low crack growth rates.

Stress corrosion crack growth behavior at the threshold stress intensity has been modeled using the salt film dissolution model developed by Danielson et al.(1). Calculations for anodic dissolution indicate that salt film formation can control crack growth behavior for extension of an intergranular stress corrosion crack enriched with an active impurity such as phosphorus or sulfur at the grain boundary. With increasing stress intensity, crack opening promotes salt film dissolution and rapid anodic dissolution at the tip. The salt film model accounts for the magnitude of the stage I-II transitions and the strong dependence of crack velocity on stress intensity. Predicted crack growth rates agree with measured rates for nickel anodically polarized to +900 mV (SCE) in 1N H_2SO_4 and tested at the threshold stress intensity.

The crack growth rate is assumed to be controlled by the rate of corrosion at the crack-tip grain boundary interface. Nickel ion transport from the tip to the bulk aqueous solution occurs during crack growth. Without stress, the corroding crevice will penetrate the grain boundary until high nickel-ion concentrations at the crevice tip cause precipitation of a salt film. When stress is applied to the sample, the crevice will open and allow nickel ion transport and dissolution of the salt film.

The schematic of the crack ion concentration and the electric potential gradients shown in Figure 3 illustrates the key features of the model. An electric potential gradient controls transport in the salt film because the film is highly resistive and because the concentration of water in the film is fixed by the solubility limit. Conversely, a concentration gradient controls transport in the aqueous solution because the concentration gradient is not fixed by the solubility limit, and because the conductive solution induces a negligible potential (IR) drop.

The electrochemical and transport equations described by Danielson et al.(1) were assumed to calculate ion concentrations in a crack aqueous solution. The time dependent transport equation for nickel ions is given by

$$dC_{Ni}/dt = D \cdot d^2C_{Ni}/dx^2 + Z_{Ni} \cdot F \cdot D \cdot d^2/dx(C_{Ni} \cdot dV/dx). \qquad (11)$$

where C_{Ni} is the nickel ion concentration, D is the ion diffusivity, F is Faraday's constant, Z_i is the ionic charge, V is the electric potential in volts, and RT is the product of the gas constant and temperature. Evaluation of the time-dependent development of the nickel ion concentration profile demonstrated that steady state is achieved after a short time compared to the experimental crack growth times.

The salt film dissolution model solves two coupled transport equations, one for the salt film and one for the aqueous solution. Boundary conditions are imposed at the grain boundary/salt film interface, the salt/solution interface, and the crack mouth as illustrated in Figure 3. The boundary condition at the grain boundary is fixed by equating the grain boundary corrosion flux and the electromigration flux flowing into the film. The porosity is assumed to be nonhomogeneously distributed. The boundary condition at the salt/solution interface is fixed by equating the electromigration flux from the salt to the Fickian flux flowing into the aqueous solution. Finally, the boundary condition at the crack mouth is fixed by a zero concentration because of dilution in the bulk aqueous solution.

The porous salt film is assumed to contain water in the pores that form a path for ion transport through the film. The porosity is assumed to be

inhomogeneously distributed. For an assumed crack opening angle dependent on the imposed stress, only one corresponding salt film thickness is consistent with the above transport equations and boundary conditions. Diffusion controls dissolution or growth of the film so that the thickness satisfies the boundary conditions described above. (19-20)

The crack geometry must be understood before the transport equations can be solved. Rice, Drugan, and Sham (21) have calculated crack opening angles for moving cracks in elastic-plastic materials. Crack opening angles are predicted to be much less for moving cracks and hence imply that stress corrosion cracks are narrower than expected from previous analyses of assumed stationary cracks. The opening for moving cracks is described as a function of crack tip plasticity and the tearing modulus, as shown:

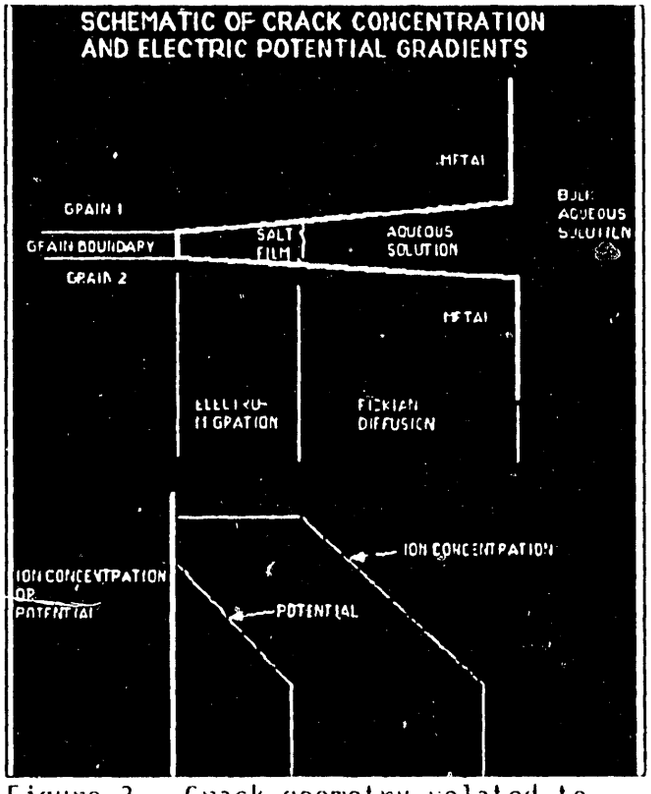

Figure 3. Crack geometry related to concentration and potential gradients in a salt film and aqueous solution. Potential drop is dominant in the salt film, whereas concentration drop is dominant in the aqueous solution.

$$\delta/r = \alpha|\sigma/E|\beta o_y/T \ln(eR/r) \qquad (12)$$

The Paris tearing modulus, T, is

$$T = (E/\sigma_o^2)\, dJ/da \qquad (13)$$

and J is the far-field value of the J-integral, and a is the crack extension. R scales as the plastic zone radius under small-scale yielding. σ_o is the yield stress, E is the elastic modulus, and β is a constant approximately equal to five. For environmental cracking, the tearing modulus can be assumed to be zero. The plastic zone radius is defined by:

$$R = e\ s\ (1-\upsilon^2)K_I^2/\sigma_o^2 \qquad (14)$$

where s and υ are a scaling constant and Poisson's ratio, respectively, and e is the natural logarithm base. The scaling constant, s, can be determined either by measurement of plastic zone size or by finite element calculation of crack tip plasticity. The measured plastic zone size is about 4 mm at the threshold stress intensity. The corresponding value of the constant, s, is 0.01.

Dean and Hutchinson (22) have calculated crack opening angles for stable moving cracks without environmental effects. Finite element equations were solved as a function of material yield stress, applied stress intensity, and strain hardening exponent to estimate the constant s. The crack tip opening angle was found to be weakly dependent on applied stress intensity, as expected from Equation (12) and (14). Based on material parameters appropriate for nickel, the crack tip opening angle is calculated to be 0.07 degrees.

The mechanics calculations for moving cracks indicate that crack tip opening angles for crack growth in nickel are expected to be small and less than 0.1 degrees, which is consistent with the measured crack opening during stage I crack growth. In contrast, mechanics calculations for stationary cracks indicate opening angles greater than 1 degree.

Prediction of Stage I Behavior in Nickel

Calculated nickel ion concentrations are shown in Figure 4a as a function of crack opening angle for a 0.1 cm-long crack with no salt film present. The salt solubility limit for nickel is shown as a horizontal line. The predictions indicate that for crack angles less than 0.07 degrees, salt precipitation is expected at the crack tip. The assumed crack length and degrees of crack opening angles are consistent with measured geometries for stage I crack growth.

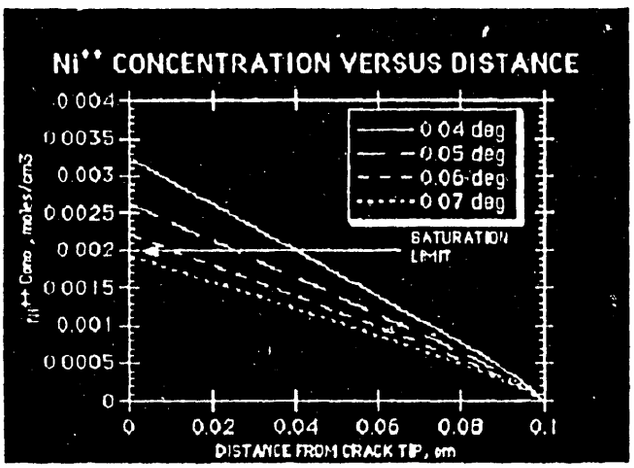

Figure 4. (a) Calculated nickel ion concentration as a function of distance from the crack tip and crack opening angle. Crack tip concentrations exceed the saturation limit for angles less than 0.07 degrees.

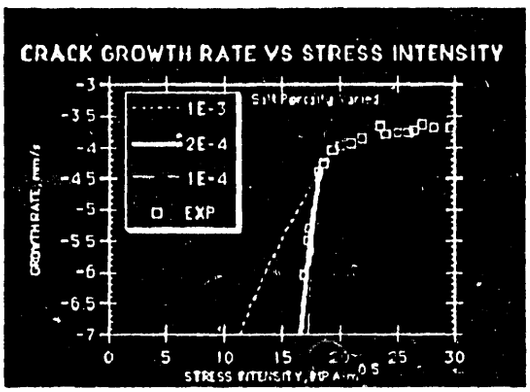

(b) Comparison of calculated crack growth rates with measured crack growth rates for indicated salt porosity. Previous models, which predict thresholds near zero, contradict the measured threshold of about 16 MPa$\sqrt{m}$.

For the salt film case, the crack tip corrosion current was calculated for the steady-state transport of nickel ions in the salt film and in the aqueous solution. Crack growth rates were calculated from the tip corrosion current for appropriate values of salt film porosity (20) and crack width at the tip. The effect of assumed stress intensity on predicted crack growth rate is shown in Figure 4b along with experimental results for Ni in 1N H_2SO_4. For a constant crack tip width of 1 nm, changing the porosity from 10^{-1} to 10^{-4} increased the slope of the growth rate versus stress intensity dependence. For a constant porosity of 10^{-3}, changing the tip width from 1 nm to 10 nm only slightly reduced the critical stress intensity for dissolving the salt film. The assumed tip width did not affect the slope of the growth rate versus stress intensity dependence.

The predicted crack growth rate is compared to the measured growth rate in Figure 4b. Assumed parameters of porosity equal to 2×10^{-4} and tip width equal to 1 nm result in excellent agreement between prediction and measurement. It is assumed that this porosity is nonhomogeneous because such a small volume fraction would not provide a continuous path if homogeneously distributed. The stress intensity was assumed to be given by the equations of Rice, Drugan, and Sham (21) and the measured size of the crack tip plastic zone. The critical crack opening angle was 0.06 degrees, which agreed with measured angles at the stage I-II transitions equal to values less than 0.1 degrees.

Discussion

A number of limitations to modeling stage I SCC were noted during the development of the crack tip chemistry model. These limitations included: 1) accurate description of the crack shape near the crack tip, 2) salt film transport parameters and processes, and 3) adequacy of experimental data.

Obtaining accurate stage I SCC data has a number of difficulties: 1) the rate of increase in da/dt with K, 2) slow crack velocities close to K_{ISCC} and the accuracy of the crack measuring apparatus, 3) crack branching or out-of-plane cracking, and 4) the effect of sample compliance and loading method. The steep slope of stage I results in greater uncertainty in the measured velocities than for the stage II regime because small changes in crack length result in large increases or decreases in crack velocity for constant load or displacement tests, respectively. Clearly, a constant K test should be used for the best accuracy, which would then be dependent on the accuracy of the load and crack length measuring systems. An accurate description of stage I requires data to be collected starting at K values very close to K_{ISCC}. The slow crack velocities near the threshold add to the uncertainty of this data because the increased amount of time needed for crack extension results in use of shorter crack extensions. Scatter in the velocity data increases with decreasing crack extensions because the crack extension reflects more of the local material microstructure and microchemistry rather than the average conditions.

Crack branching occurs when da/dt is independent of K, as in stage II. This becomes a problem near the transition from stage I to stage II but should not be a problem for K values near K_{ISCC}. Likewise, the problem of out-of-plane cracking increases with increasing K. Both crack branching and out-of-plane cracking increase the uncertainty between the far field and crack tip K values and therefore increase the uncertainty of the da/dt-K relationship. Sample compliance effects are primarily a concern in comparing data from different sample types but it should, in principle, be

possible to correlate this type of data if the compliances of the samples are known. It should also be possible to correlate comparisons between experimental and theoretical calculations if the compliance of the samples are known. Differences in sample loading method can also produce different slopes in the stage I regime. Programmed increasing or decreasing loads result in different slopes than a constant COD/load shedding approach. Again, these should, in principle, be correlatable if sufficient information about sample compliance and loading method is known. In general, this type of information is not provided so it is difficult to make use of much of the existing data on stage I da/dt-K.

The salt film dissolution model for K_{ISCC} and stage I behavior could be applicable to materials other than the Ni-P system. Complementary theories have been presented by Parkins and Humphries (23) and Conor (24). These authors suggested that K_{ISCC} was dependent on the crack opening rate being sufficient to expose the crack tip in the presence of a corrosion product. The ideas of Parkins and Humphries and of Conor describes K_{ISCC} as only being due to a blockage of the crack tip from corrosion product along the crack walls.

It is also interesting to consider the applicability of the salt film dissolution model to IGSCC of sensitized stainless steel where the wall corrosion rate is controlled by the Cr concentration. The Cr concentration of the crack wall would be a function of distance from the crack tip since the crack wall would corrode back to higher Cr concentrations when exposed to the electrolyte. Also, varying sensitization conditions produce different grain boundary Cr profiles and thus should produce different K_{ISCC} and stage I behavior. A correlation between Cr profile and K_{ISCC} and stage I for stainless steel would be a good test of the salt film model; however, data sufficient to test this concept is not available. Another critical test could be to vary the wall corrosion rate by varying the electrolyte chemistry. An example would be the addition to the electrolyte of an anion that degrades passivity for a material undergoing active-path IGSCC, such as Ni-P. Tests with passive film forming material, such as stainless steel, could be misleading because of the simultaneous effect of the anion on passive film stability at the crack tip and the crack wall.

The salt film dissolution model is not embodied in any of the SCC models given in Table 2. The model by Andresen is for passive film rupture and seems to describe stage II K dependence. Rupture of the salt film at the crack tip could be considered comparable to rupture of the passive film; however, the K dependence given by equation 2-1 is not typical of most stage I da/dt-K slopes. Also, the model presented by Newman, equation 2-2, describes crack extension by fracture of a thick corrosion product. The salt film is physically distinct from a corrosion product; therefore, these two models are distinctly different.

The variable K dependence given by equation 2-3 proposed by Vermilyea (16) describes the strong K dependence in stage I given that η is very small. In this model, Vermilyea suggested that the generation by hydrolysis of a species such as protons was critical to crack growth and that as the difference in concentration between the tip and the bulk solution increased η decreased. This concept can be reversed to consider critical anion species such as Cl^- where the value of η decreases with increasing concentration of the anion at the crack tip. Increasing concentrations of anions that promote passive film breakdown on the crack walls would require greater crack opening to obtain a comparable salt film dissolution and hence produce a decrease in the slope of the da/dt-K relationship in stage I. Equation 2-3 predicts an increase in the exponent m because of a

decrease in η with increasing concentrations of a critical species. As noted previously, there is a trend where m exhibits a dependence on the type and concentration of anion. A further evaluation of the effects of a critical anion species such as Cl- on the salt film dissolution model is warranted.

The model presented by Macdonald and Urquidi-Macdonald (17) also contains elements that are comparable to the salt film dissolution model. However, Equation 2-4 considers the crack tip potential being controlled by the balance of positive ion current produced by the crack with the reduction of oxygen at the external crack surfaces. Passive film rupture is considered to control the crack tip corrosion rate. In the salt film dissolution model, the crack tip potential is controlled by the resistive salt film in stage I and not by the balance in positive and negative currents.

The chemical reaction rate models by Lee and Tromans (9) and by Freiman (18) are not consistent with the salt film dissolution model. These models consider the chemical reaction rate as controlling the crack velocity where the salt film dissolution model considers transport through the resistive salt film as controlling the crack velocity in stage I. Stage II behavior could be accurately characterized by a chemical reaction rate model or by a crack tip electrolyte transport model, but stage I behavior does not appear to be limited by these processes.

Summary

A comparison between experimental stage I SCC behavior with models of SCC containing stress intensity dependence has shown that this aspect of SCC is not correctly described by these models. An exception to this is the salt film dissolution model developed for IGSCC of Ni-P described in this paper. This model correctly predicts the $K_{I_{SCC}}$ and the stage I slope and the stage I-II transition for IGSCC of Ni tested in 1N H_2SO_4 for certain salt film characteristics. Other models do not predict the $K_{I_{SCC}}$ or the stage I slope. A correct description of stage I behavior will necessarily lead to a better understanding of SCC mechanisms since this stage is the critical link between $K_{I_{SCC}}$ and the steady state stage II cracking regime. Also, more quantitative descriptions of stage I behavior will also improve our ability to predict the life of a component in a SCC environment.

Acknowledgment

This research was supported by the Office of Basic Energy Sciences, Division of Materials Sciences of the U.S. Department of Energy under Contract DE AC06-76RLO 1830.

References

1. M. J. Danielson, C. A. Oster and R. H. Jones, Corrosion Science, Vol. 32 (1991) p. 1.

2. R. H. Jones, M. J. Danielson, and D. R. Baer, in Corrosion of Nickel-Base Alloys, Journal of Materials for Energy Systems, Vol. 18, 1986, pp. 185.

3. F. P. Ford, in Embrittlement by the Localized Crack Environment, R. P. Gangloff, Ed., TMS AIME, Warrendale, Pa., 1984, pp. 117-148.

4. M. O. Speidel, EPRI NP-2531, Electric Power Research Institute, Palo Alto, Calif.

5. R. C. Newman, K. Sieradzki, and H. S. Isaacs, Metallurgical Transactions, Vol. 13A, 1982, pp. 2015.

6. P. Chung, A. Yoshitake. G. Cragnolino, and D. D. Macdonald, Paper No. 166, Corrosion/84, New Orleans, La., 1984.

7. M. O. Speidel, in Predictive Capabilities in Environmentally Assisted Cracking, R. Rungta, Ed., 1985, American Society of Mechanical Engineers, New York, pp. 443.

8. D. Singbeil, and D. Tromans, Metallurgical Transactions, Vol. 13A, 1982, pp. 1091.

9. L. D. Lee and Tromans, D., in Environment-Sensitive Fracture of Engineering Materials, Z. A. Foroulis, Ed., TMS-AIME, Warrendale, Pa., 1979, pp. 232-240.

10. R. H. Jones, M. A. Friesel and W. W. Gerberich, Metall. Trans.A, Vol. 20A, (1989), p. 637.

11. R. H. Jones, B. W. Arey, D. R. Baer and M. A. Friesel, Corrosion, Vol. 45, (1989) pp. 494.

12. R. H. Jones, B. W. Arey, C. F. Windisch and D. R.Baer, Corrosion, Vol. 47 (1991) p. 542.

13. P. L. Andresen and F. P. Ford, Matl. Sci. and Eng., A103 (1988) P. 167.

14. F. P. Ford, EPRI NP 2589, Electric Power Research Institute, Palo Alto, CA, 1982.

15. J. F. Newman, Corrosion Science, Vol. 21, 1981, pp. 487.

16. D. A. Vermilyea, in Stress Corrosion Cracking and Hydrogen Embrittlement of Iron Base Alloys, R. W. Staehle, J. Hochmann, R. D. McCright and J. E. Slater, Eds., 1973, National Association of Corrosion Engineers, Houston, TX, pp. 208-217.

17. D. D. Macdonald and M Urquidi Macdonald, Corrosion Science, Vol. 32 (1991) p. 51.

18. S. W. Freiman, J. Geophysical Res., Vol 89 (1984) p. 4072.

19. J. W. Tester and H. S. Isaacs, J. of the Electrochemical Soc., Vol. 122, (1978) p. 1438.

20. M. J. Danielson, "Transport Properties of Salt Films on Nickel in 0.5N HCl," J. of the Electrochemical Soc., Vol. 135, No. 6, 1988, pp. 1326-1332.

21. J. R. Rice, W. J. Drugan, and T-L. Sham, "Elastic-Plastic Analysis of Growing Cracks," Fracture Mechanics: Twelfth Conference, ASTM STP 700, American Society for Testing Materials, 1980, pp. 189221.

22. R. H. Dean and J. W. Hutchinson, "Quasi-Static Steady Crack Growth in Small-Scale Yielding," Fracture Mechanics: Twelfth Conference, ASTM STP 700, American Society for Testing Materials, 1980, pp. 383-405.

23. R. N. Parkins and M. J. Humphries, Proc. Int. Conf. Fundamental Aspects of Stress Corrosion Cracking, R. W. Staehle, ed. National Association of Corrosion Engineers, Houston, Texas, p. 384.

24. P. C. Conor, Corrosion, Vol. 43 (1987) p. 614.

END

DATE
FILMED
2/04/92